工學碩士學位論文

Enhanced antimicrobial activity of silver/polyrhodanine composite decorated silica nanoparticle

은/폴리로다닌 복합체를 함유한 실리카 나노입자의 항균 증진 효과

2013年 2月

서울大學校 大學院
化學生物工學部
金 炫 伶

Abstract

Enhanced antimicrobial activity of silver/polyrhodanine composite decorated silica nanoparticle

Hyunyoung Kim

School of Chemical and Biological Engineering

The Graduate School

Seoul National University

This work describes the novel solution system synthesis of silver/polyrhodanine composite decorated silica NPs. Polymerization of polyrhodanine proceeded preferentially on the surface of the silica NPs where the Ag+ ion was located. During the polymerization, the embedded Ag^{+} ions reduced to metallic Ag NPs and consequentially silver/polyrhodanine composite NPs (*ca.* 7 nm) were formed on the surface of the silica nanoparticle. The existence of silver NPs and polyrhodanine on the silica NPs were verified through microscopic observation, FTIR, UV-vis, and XRS analysis. The composite nanoparticle decorated silica NPs exhibited excellent antimicrobial activities against Gram-negative *Escherichia coli* and Gram-positive *Staphylococcus aureus*. Importantly, the synthesized composite NPs retained antimicrobial activity under silver depletion condition due to the contact-active biocidal polyrhodanine. Therefore, it can be anticipated that the

silver/polyrhodanine composite decorated silica NPs have potential for use as a long-term antimicrobial agent.

Keywords: Silver nanoparticle, Polyrhodanine, Nanocomposite, Oxidation polymerization, Bactericidal.
Student Number: 2011-22915

Contents

List of Tables

List of Figures

Chapter 1. Introduction

1.1 Background of antimicrobial field

Although human mortality from bacterial infections has decreased over the last century due to developments in medical science, these remain the number one cause of death.[1] A large number of bacterial infections originate from viable bacteria that adhere to implants and medical devices.[2,3] When bacteria attach to a material surface and cell numbers increase, they start to form a biofilm. After developing on a surface, this biofilm is extremely difficult to remove and allows microbial cells to survive even under harsh conditions. In contrast to planktonic (free-floating) bacteria, the bacteria in biofilms are up to 1000 times more tolerant to antibiotics and other biocides.[4,5] Thus, inhibition of biofilm formation is considered to be the most important goal in antimicrobial research. To do this, it is necessary to inhibit the early stages of bacterial adhesion. In general, this can be achieved by either killing the planktonic bacteria prior to adhesion using biocides, or by modifying surface properties to inhibit bacterial adhesion.

During the last decades, numerous effective bactericidal materials that inhibit bacterial growth have been developed. Especially, the field of antimicrobial polymers has great advances in terms of efficacy enhancement, control of size and morphology, and synthetic route development.

1.2 Antimicrobial nanomaterials

1.2.1 Silver nanoparticles

Various antimicrobial agents have been developed for curing and preventing diseases in public health hygiene and antifouling in biomedical industry.[6-8] Among them, silver nanoparticle which release Ag^+ ions has been recognized as an excellent antimicrobial agent due to their effective biocidal ability and non-toxicity to human cells.[9-11] Possible mechanism of killing microorganism by silver ion may be explained as following hypotheses: 1) silver ion inhibits the ATP synthesis via binding formation with ATP synthesis enzyme molecules in the cell wall, 2) silver ion enters the cell and binds with DNA, leading to the DNA denaturation, 3) silver ion blocks the respiratory chain of microorganism in the cytochrome oxidase and NADH-succinate-dehydrogenase region.[12]

1.2.2 Antimicrobial polymer nanomaterials

To fabricate ecologically sound and long-lasting antimicrobial agents, non-leaching (contact-active) antimicrobial polymers have been designed. It is well known that bacterial cells generally have a net negative charge at their surface due to the teichoic acids of the Gram-positive bacterial cell wall and the phospholipids within the outer membrane of Gram-negative bacteria.[13,14] Based on these features, cationic polymers that can interact with negatively charged bacterial membranes have been intensively investigated as efficient antimicrobial materials.[13-16] Although the exact mechanism underlying the interactions between membrane-active biocidal polymers and bacterial cells remains unclear, membrane-disruption is broadly accepted as the bactericidal mechanism of cationic polymers.[15-17] Although contact-active polymers have some advantages, such as long-term durability, being ecologically sound, and prevention of resistance, their moderate antimicrobial efficiency compared with release-type biocides is in need of improvement.[18] The size of antimicrobial agents has been

demonstrated to be a key factor in their efficacy.[19-21] In other words, biocidal efficiency depends on the exposed active area of the biocide. During the last decade, nano-sized antimicrobial particles have been reported to display enhanced antimicrobial activity against typical bacteria when compared with their bulk counterparts.[20-23]

1.3 Metal/polymer nanocomposites

1.3.1 Antimicrobial silver-polymer nanocomposite

Although not fatal, silver nanoparticles have shown toxicity toward mammalian cells.[24,25] The toxicity of colloidal silver nanoparticles has been attributed to uptake of silver nanoparticles by cells or to the oxidative release of silver cations from the surface of the silver nanoparticles that can affect basic functions in mammalian cells.[26] From this viewpoint, immobilization of nanosilver onto adequate substrates is advantageous because it inhibits direct uptake of the nanoparticles by cells. In addition, compared to colloidal silver nanoparticles, immobilized silver nanoparticles effectively resist oxidation and aggregation, which can reduce the

antibacterial efficiency.[27,28] There are numerous reports on the silver nanocomposites and their antibacterial performances.[27-30] For example, Lu *et al.* reported that silver nanoparticles embedded into silicon nanowires are much more stable and resistant to aggregation than colloidal silver nanoparticles.[28] The antibacterial performance is time-limited in silver containing materials that kill bacteria *via* the release of silver ions or silver nanoparticles.[28,31] To improve the durability of biocidal activity, researchers have suggested incorporation of silver into biocidal polymers.[31-33] Therefore, composites of the polymers with silver nanoparticles are promising for long-term and efficient antimicrobial performance. For example, Rubner *et al.* reported a dual-functional bactericidal coating based on a two-level coating of quaternary ammonium silane and silver.[31] These composites maintained antibacterial performance even after the contained silver was depleted.

1.3.2 Preparation strategies

A variety of solution-phase methods for preparation of metal or inorganic nanostructures have been developed.[34-36] However, solution-phase synthesis of

polymer nanostructure remains limited. As mentioned above, nanometre-sized polymers are unstable and readily revert to the bulk state. To overcome these problems, solution-phase synthesis of metal-polymer complex nanostructures was introduced which uses the coordination activity between metal binding groups of polymer and metal ions (or metal nanoparticles) as a driving force. In these methods of synthesis, the polymer can be fabricated at a submicron size because the metal provides mechanical stability to the composite nanostructure. Among the metal compounds, silver has been investigated extensively due to its stability and excellent antimicrobial activity.[37,38] Use of silver cations as an initiator of oxidative polymerization is well known, particularly in the field of conductive polymers, such as pyrrole or aniline.[39-41] When silver ions participate in this reaction, they are simultaneously reduced to zero-valent metallic silver nanoparticles. Although the number of possible monomers is limited due to the high oxidation potential of Ag(I) (E = 0.8 V), the use of the silver ion as an initiator of oxidative polymerization is facile synthetic route for silver nanoparticle-impregnated polymers.

1.4 Objective of this study

The aim of this work is providing synthetic strategies for silver/polyrhodanine nanocomposite with enhanced antimicrobial activities. To do this, silica nanoparticle with *ca.* 50 nm of diameter were employed as substrate for anchoring of silver ions. The facile oxidation polymerization of polyrhodanine proceeded on the silver ions anchored silica surface. The long-term antimicrobial properties of the synthesized nanocomposite particles were systematically investigated against Gram-negative *Escherichia coli* and Gram-positive *Staphylococcus aureus*.

Chapter 2. Experimental

2.1 Materials

Silica NPs with diameters of ~50 nm were synthesized using tetraethyl orthosilicate (TEOS) and ammonia solution (28-30 %) as typical method. (3-mercaptopropyl)trimethoxy silane was purchased from Aldrich (Milwaukee, WI, USA) and used as silane coupling agent for modification of silica surface. Rhodanine monomer, silver nitrate (99 %), ethylene glycol, 1-,6-hexanediamine, and ethanol were used which were purchased from Aldrich (Milwaukee, WI, USA). As a silver ion scavenger, sodium thiosulfate and sodium thioglycolate were obtained from Aldrich. To test bacterial growth, *E. coil* (ATCC 11775) and *S. aureus* (ATCC 12600) were purchased from The Fisher Company (Tucson, AZ, USA).

2.2 Fabrication of silver/polyrhodanine composite decorated silica nanoparticles

To prepare silver/polyrhodanine composite decorated silica NPs (SiO_2-Ag/PRh NPs), 50 nm silica was pretreated with thiol-functioned silane. The 300 mg of silica was dispersed in 3 mL of ethanol solution to which 120 μL of (3-mercaptopropyl)trimethoxy silane and 150 μL NH_4OH (30 %) solution was added, and the solution was vigorously stirred at room temperature for 24 h. After centrifugation, thiol-treated silica NPs were obtained and dried in a vacuum oven at 25 °C. Then, 50 mg of thiol-silane treated silica NPs was dispersed in 30 mL of ethanol by sonication for 20 min. Silver nitrate (0.188 mmol) was introduced to the reactor and stirred for 2 h at 60 °C. After then, rhodanine monomer (0.075 mmol) was introduced to the reaction medium and the chemical oxidation polymerization of rhodanine proceeded for 24 h on the surface of silica NPs at 60°C with vigorous stirring. After polymerization, Ag/PRh decorated silica NPs were obtained by centrifugal precipitation and washed with excess ethanol to remove residual reagents.

2.3 Fabrication of silver decorated silica NPs

To prepare SiO_2-Ag NPs, silver nitrate (0.177 mmol) was previously dissolved in 30 mL of ethylene glycol. After the silver nitrate completely dissolved in the solution, previously thiol-silane treated silica (30 mg) was added and vigorously stirred at room temperature for 1 h. Then, 1,6-hexanediamine 0.5 mg was added as reducing agent. After reaction for 1 h at 25 °C, Ag NPs decorated silica NPs were obtained by centrifugal precipitation and washed with excess ethanol to remove residual reagents.

2.4 Antimicrobial test

E. coli and *S. aureus* were cultivated in sterilized Luria–Bertani (LB) broth and then incubated overnight at 37 °C in a shaking incubator. The microorganism suspensions used for the tests contained 10^6–10^7 colony-forming units (CFU) in 1 mL. For the bacterial test, as-prepared NPs (5 mg) were dispersed in 1 mL of sterile water and inoculated with 10^5-10^6 CFU of bacteria(*E. coli* and *S. aureus*). The bacteria-inoculated solutions were incubated in a shaking incubator at 37 °C. After 1h of contacting time, the

same volume of each solution were taken from each tube and cultured on LB agar plates. The LB agar plates were kept at 37 °C for 24 h and the grown bacterial colonies was observed to evaluate antibacterial performance. The bacterial survival was calculated as bacterial survival = (B/A × 100) (where A is the number of surviving bacteria colonies in the control and B is that in the sample).

2.5 FE-SEM observation of bacteria

The SiO_2-Ag/PRh NPs were hydraulically pressed to obtain a disc. Then, the bacterial suspension was drop-casted on the surface of the sample disc and cultivated at 37°C for 4 h. The bacteria were then fixed in 2.5% glutaraldehyde for 2 h and rinsed several times with distilled water. Post-fixation proceeded for 1 h with 1% osmium tetroxide in distilled water. After fixation, the samples were dehydrated with ethanol (20–100%), air-dried, and sputter-coated with platinum/palladium for FE-SEM observation.

2.6 Antimicrobial test under silver depletion condition

In order to observe the long-term antimicrobial activity of synthesized composite NPs, antimicrobial test was performed under silver depletion condition using silver ion scavenger. For the test, as-prepared SiO_2-Ag/PRh NPs (5 mg) were dispersed in 1 mL of distilled water and neutralized with 100 μL of a neutralizer solution (14.6 wt% sodium thiosulfate and 10 wt% sodium thioglycolate in distilled water). The prepared neutralizer solution has been known as silver ion scavenger.[42] In order to exclude the antimicrobial activity of silver NPs, excess amount of neutralizer solution was used. After 30 min of shaking, the samples were inoculated with 10^5 to 10^6 CFU of bacteria (*E. coli* and *S. aureus*). A blank solution, pristine silica NPs, thiol-silane treated silica NPs, and silver NPs decorated silica (SiO_2-Ag) NPs were also prepared as an experimental control. The bacteria-inoculated solutions were incubated in a shaking incubator at 37 °C. After 1 hour, the same amount of aliquots were taken from each tube and cultured on LB agar plates. The LB agar plates were kept at 37 °C for 24 h and the number of bacterial colonies was counted to evaluate antibacterial

performance.

2.7 Characterization

Transmission electron microscopy (TEM) images were obtained with a JEM-200CX (JEOL, Japan) at an acceleration voltage of 200 kV. Field-emission scanning electron microscopy (FE-SEM) images were obtained using a JEOL 6700 at an acceleration voltage of 10 kV. To prepare samples for TEM and FE-SEM characterization, the prepared NPs were dispersed in water and cast onto a copper grid and silicon wafer, respectively. Fourier transform infrared (FTIR) spectra were obtained using a Bomem MB 100 spectrometer (Quebec, Canada) in absorption mode at a resolution of 4 cm−1 by averaging 64 scans. Ultraviolet–visible (UV–Vis) spectra were acquired using a Lambda-20 spectrometer (PerkinElmer, USA). To obtain UV–Vis spectra, the samples were dissolved in N-methyl-2-pyrrolidone. X-ray photoelectron spectroscopy (XPS) data was obtained using Sigma Probe electron spectroscope.

Chapter 3. Results and discussion

3.1 Fabrication of SiO_2-Ag/PRh NPs

To prepare SiO_2-Ag/PRh NPs, silica NPs were pretreated with thiol-functionalized silane. Through the silane treatement, thiol functionalized silica NPs(SiO_2-thiol) which have strong affinity for metal ions were prepared.[43] Then, the SiO_2-thiol were dispersed in silver nitrate dissolved ethanol solution. The Ag(I) ions preferentially attached to the silica surface due to strong metal binding property of thiol-functional groups on the silica NPs. Rhodanine monomer was introduced to the reaction medium and the Ag(I) ions initiated the chemical oxidation polymerization of rhodanine. Because Ag(I) ions attached on the surface of silica NPs, the polymerization proceeded preferentially on the silica surface. During the oxidation polymerization, Ag(I) ions reduced and silver NPs were formed on the silica NPs simultaneously.[32,33] After polymerization, Ag/PRh decorated silica NPs with dark brown color, which represents the existence of polyrhodanine, were obtained.

3.2 Characterization of SiO_2-Ag/PRh NPs

3.2.1 Microscopic analysis

TEM images in Figure 1 present the morphology of the synthesized SiO_2-Ag/PRh NPs. As shown in the TEM images (Figure 1a, b), the silver/polyrhodanine particles were densely loaded on the surface of silica NPs after the reaction; the average diameter of the loaded particles was approximately 7 nm. Additionally, the loaded particles were analyzed by HR-TEM (Figure 2). The measured lattice fringe spacings of 0.23 nm in the loaded particles correspond to the (111) crystal planes of silver NPs.[44] Notably, the lattice fringe of the silver NPs is blurred in HR-TEM observation, especially the edges of the loaded particles. It may be suggested the polyrhodanine exists on the silver NPs and dims the fringe.

The silver NPs decorated silica NPs were also synthesized as comparative materials in antimicrobial test. In the preparation, we use 1,6-hexanediamine as an reducing agent instead of rhodanine monomer. As shown in Figure 3, silver NPs loaded silica NPs were successfully prepared; the average diameter of the silver NPs was about 4 nm.

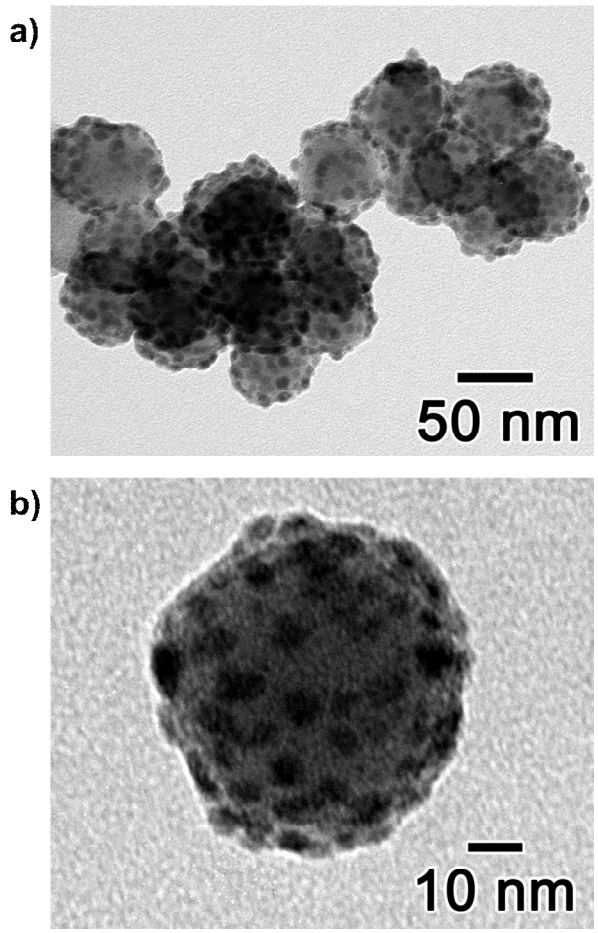

Figure 1 (a) Low- and (b) high-magnified TEM images of synthesized silver/polyrhodanine composite decorated silica NPs.

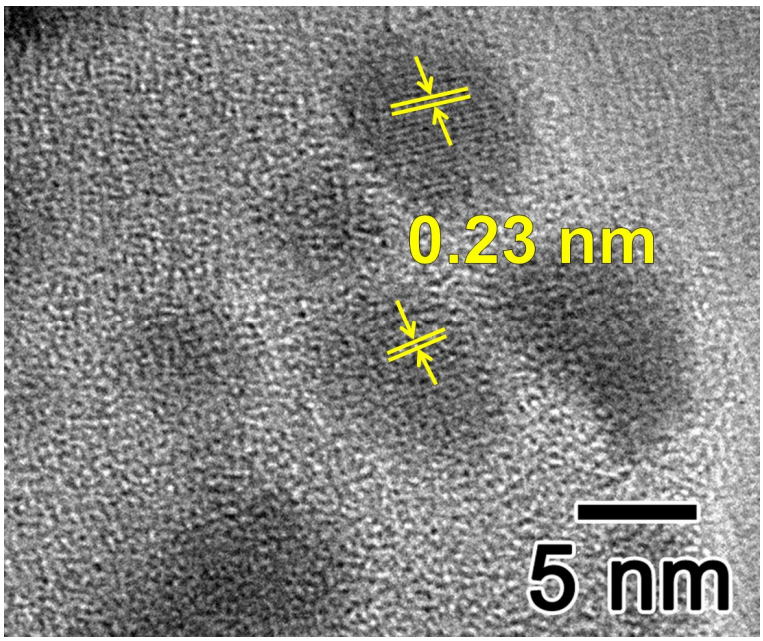

Figure 2 HR-TEM images of synthesized silver/polyrhodanine composite decorated silica NPs.

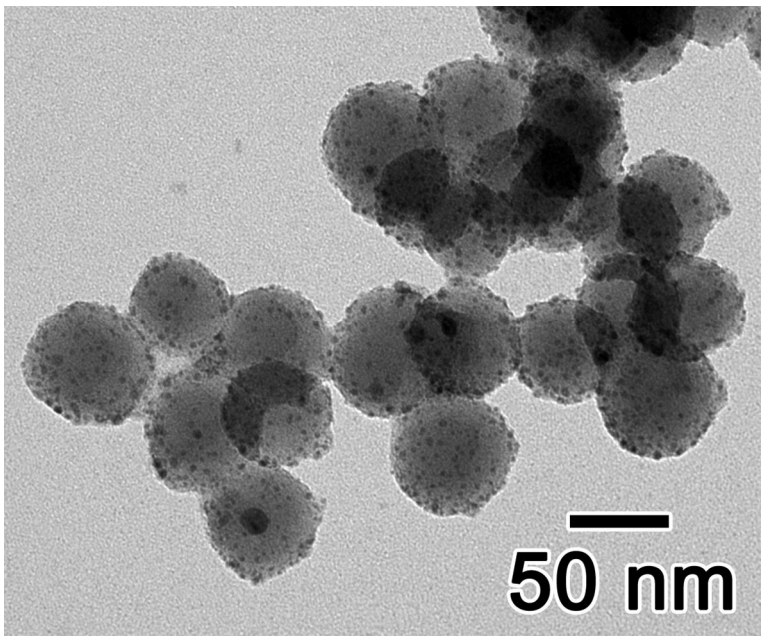

Figure 3 TEM images of silver NPs decorated silica NPs.

3.2.2 XPS analysis

An XPS analysis was performed to confirm the existence of the silver nanoparticle on the silica NPs. In general, metallic silver 3d peaks are centered at 368 eV (for Ag $3d_{5/2}$) and 374 eV (for Ag $3d_{3/2}$), with a spin energy separation of 6.0 eV.[45,46] As shown in the Figure 4, as-prepared SiO_2-Ag/PRh NPs present two sharp peaks at 368 eV and 374 eV, with a 6.0 eV separation, corresponding to the Ag $3d_{5/2}$ and Ag $3d_{3/2}$ binding energies, respectively. It can be observed that the SiO_2-Ag/PRh NPs had same spin energy separation as metallic silver with negligible shifts, which means the zero-valent silver NPs were formed after the oxidation polymerization of polyrhodanine.

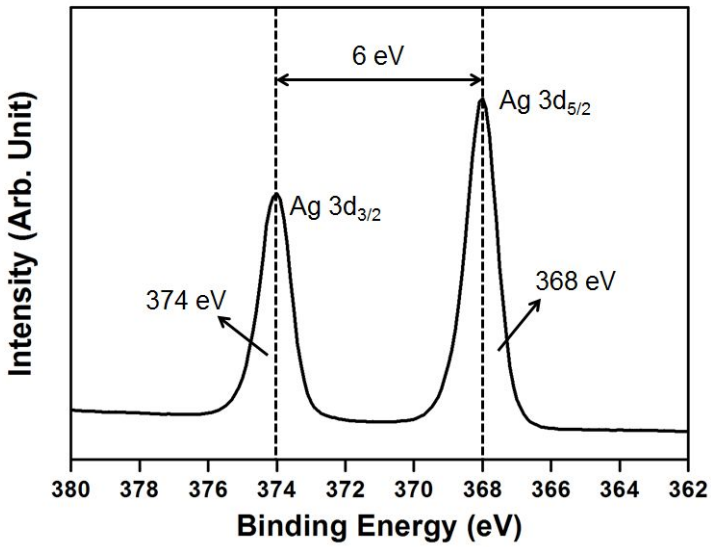

Figure 4 XPS spectrum of Ag/PRh nanoparticle decorated silica NPs.

3.2.3 FTIR and UV-vis analysis

FTIR and UV-vis spectroscopy of as-prepared samples were observed to verify the polymerization of rhodanine. In FTIR spectrum of SiO_2-Ag/PRh NPs (Figure 5), strong peak at 1710 cm^{-1} attributed to the C=O stretching of rhodanine monomer is disappeared and new peaks at 1638, 1560, and 1182 cm^{-1} are observed. The absorbance peak at 1638 cm^{-1} is assigned to the C=C stretching vibration, and the peak at 1560 cm^{-1} is originated from $C=N^+$ stretching of the conjugated polyrhodanine. In addition, the $C–O^-$ stretching peak at 1182 cm^{-1} is also obtained.[32,33] The characteristic peaks of rhodanine monomer and polyrhodanine are arranged in Table 1. Based on the FTIR spectra, it can be proposed that the polymerization of rhodanine proceeded over carbon and nitrogen atoms as proposed in Figure 6. The oxidation process includes the steps of monomer oxidation over amino group with cation-radical formation and its coupling accompanied by deprotonation. In the further oxidation steps, a rearrangement takes place and one more time deprotonization occurs.[47] The oxidation polymerization mechanism and the oxidized polymer form are presented in Figure 7.

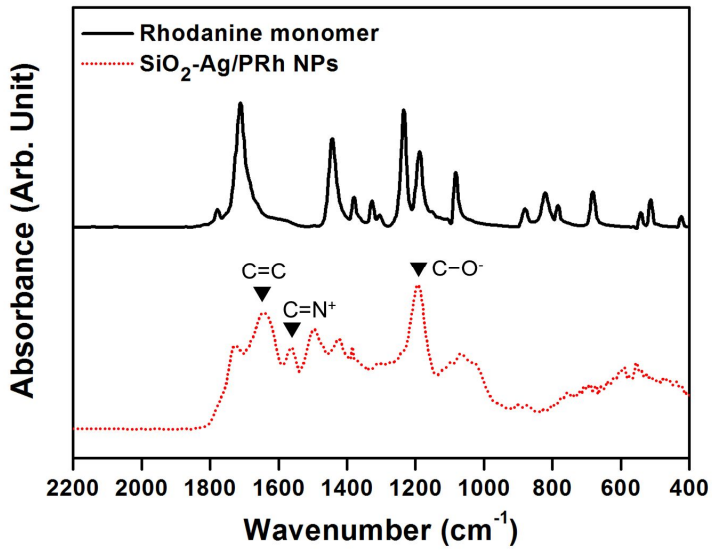

Figure 5 FTIR spectra of rhodanine monomer (black line) and Ag/PRh nanoparticle decorated silica NPs (red dot).

Table 1. FTIR assignment of rhodanine monomer and polyrhodanine

Materials	Wavenumber[a]	Assignments
Rhodanine monomer	1710	C=O stretching
Polyrhodanine	1638	C=C stretching
	1560	$C=N^+$ stretching
	1182	$C-O^-$ stretching

[a] unit: cm^{-1}

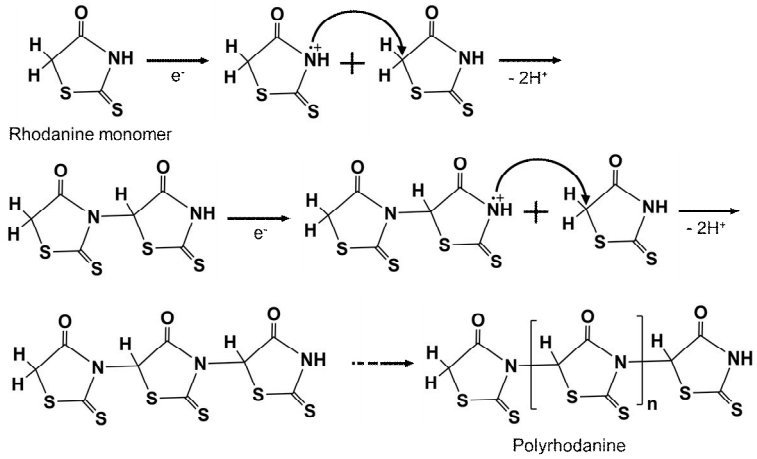

Figure 6 Schematic illustration of oxidation polymerization mechanism of polyrhodanine

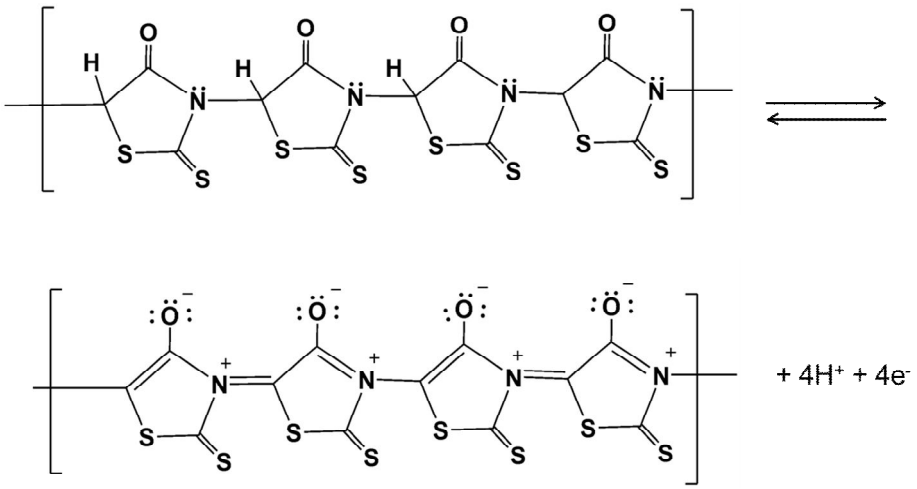

Figure 7 Schematic illustration of further oxidation step of polyrhodanine

The UV-vis spectrum analysis of the synthesized NPs also supports successful polymerization of polyrhodanine (Figure 8). Before the polymerization, the rhodanine monomer shows an absorption peak at around 380 nm, which is attributed to an n–p* transition of rhodanine monomer.[47] On the other hand, As-prepared sample showed absorption peaks at 420 and 465 nm and peak at 380 nm is disappeared. The absorption peak at 420 nm may be attributed to the red-shifted n–p* transition of rhodanine due to silver-binding complex structures. Importantly, the peak observed near 465 nm is due to the polymeric backbone of synthesized polyrhodanine.[32,33,47] Based on the spectra analysis, it is concluded that the oxidation polymerization of rhodanine was successfully proceeded using silver ions as initiator.

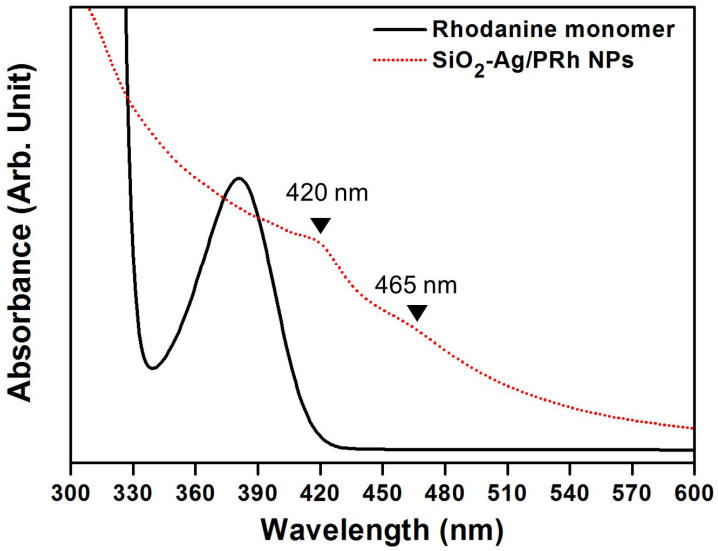

Figure 8 UV-vis spectra of rhodanine monomer (black line) and Ag/PRh nanoparticle decorated silica NPs (red dot).

3.2.4 Synthetic mechanism of SiO_2-Ag/PRh NPs

When rhodanine monomer was added, we found that in the polymerization system, what formed are silver/polyrhodanine nanocomposite NPs on the surface of the silica. Obviously, SiO_2-thiol plays an important role here. In our previous work, silver/polyrhodanine composite nanotubes were synthesized under the same condition as in Figure 1 except for the existence of silica NPs.[32] A formation mechanism of silver/polyrhodanine composite NPs on the surface of the SiO_2 NPs is that the silver ions were anchored on the thiol-silane treated silica NPs because thiol-group has strong affinity to metal ions. Then, Newly added rhodanine monomer preferentially polymerized on the SiO_2-thiol because of the high concentration of silver ions. Silver ions initiated oxidation polymerization of rhodanine, at the same time silver ions were reduced to the metallic Ag NPs as schematically illustrated in Figure 9. As a result, Ag/PRh nanocomposite decorated silica NPs were formed.

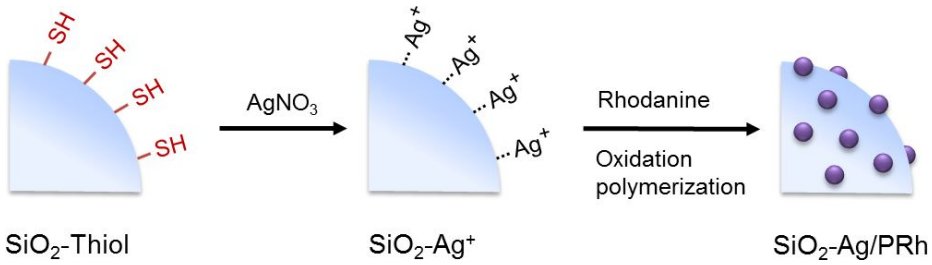

Figure 9 Schematic illustration of the formation mechanism of Ag/polyrhodanine nanocomposite on the surface of SiO2 NPs

3.3 Antimicrobial activity of SiO_2-Ag/PRh NPs

3.3.1 Antimicrobial activity of SiO_2-Ag/PRh NPs

The synthesized SiO_2-Ag/PRh NPs were expected to exhibit synergetic antibacterial activity due to the decorated silver and polyrhodanine. To evaluate the bactericidal activities of the SiO_2-Ag/PRh NPs, Gram-negative *E. coli* and Gram-positive *S. aureus* were used as test bacteria. The 5 mg of sample was dispersed in 1 mL of distilled water and inoculated with 10^5-10^6 CFU of bacteria. After 1 h of contacting time, the same volume of the each solution was cultured on LB agar plates. As shown in Figure 10, after 24 h of incubation, densely grown bacterial colonies were observed on the control (untreated) LB agar for both *E. coli* (Figure 10a) and *S. aureus* (Figure 10c). On the other hand, the SiO_2-Ag/PRh NPs treated bacterial solution exhibited no-growth of bacterial colony, which indicates excellent antibacterial activity against both bacteria (Figure 7b and 7d). The morphological changes in bacteria after SiO_2-Ag/PRh NPs treatment were observed using FE-SEM. Intact *E. coli* had a rod-like shape (Figure 11a), whereas *S. aureus* was spherical shape (Figure 11c). After contact with the SiO_2-Ag/PRh, *E. coli*

had been damaged to its outer membrane and shrunk compared with intact form (Figure 11a and 11b). Similarly, *S. aureus* also showed shrunk morphology, which represents it had been damaged to its membrane after contact with the synthesized biocides (Figure 11c and 11d). These results suggest that the SiO_2-Ag/PRh NPs have effective bactericidal properties.

Polyrhodanine has tertiary amide groups in its polymer structure. The tertiary amide groups in the NPs could be partially protonated in aqueous conditions and developed a positive charge.[23] The positively charged parts of the polyrhodanine shell interacted with the lipid bilayer structures of the bacteria membranes, leading to the destruction of the membrane.[23,32,33] Meanwhile, silver nanoparticle has been well known as excellent antimicrobial agent. Thanks to the numerous research groups, it is verified that the silver nanoparticle provides excellent antimicrobial activities *via* releasing a cationic silver ions to approaching bacteria.[9-12] In this work, the synthesized SiO_2/PRh NPs present enhanced antimicrobial effects based on the bactericidal properties of decorated Ag and polyrhodanine nanocomposite.

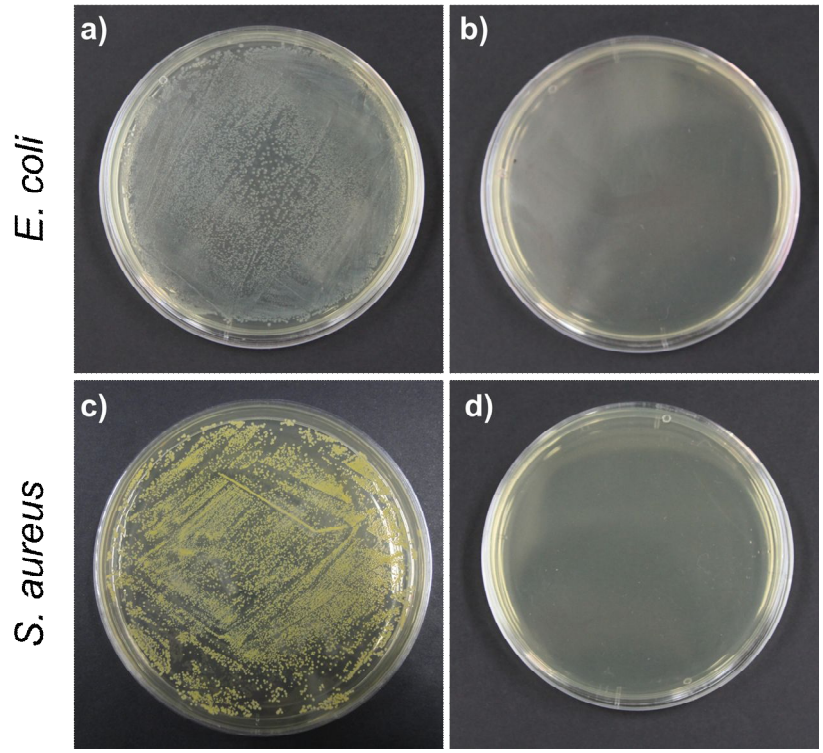

Figure 10 Photographs of bacterial colonies formed by *E. coli* (top) and *S. aureus* cells (bottom) (left) in the absence of bacteriocidal agents (control experiment) and (right) treated with the silver/polyrhodanine decorated silica NPs for 1 h.

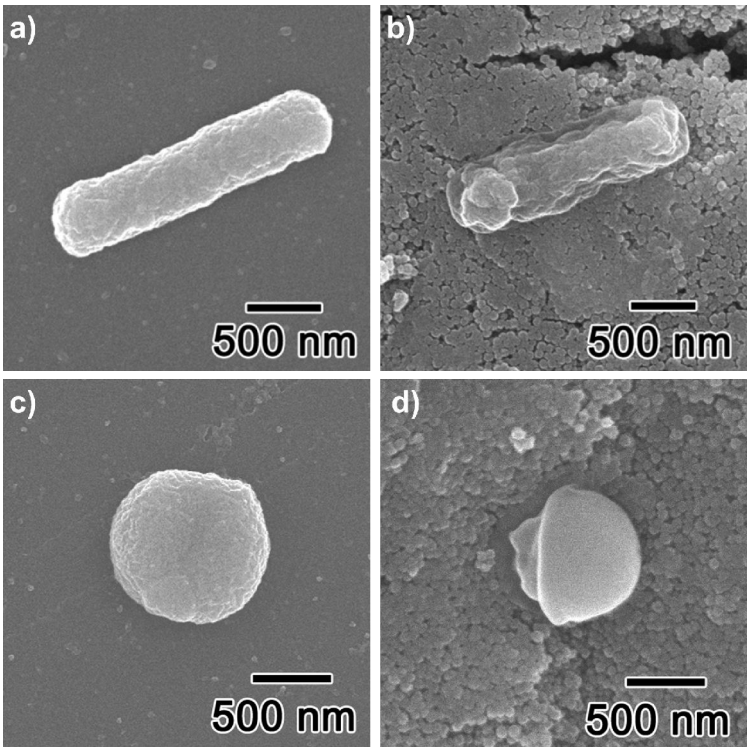

Figure 11 FE-SEM images of *E. coli* (top) and *S. aureus* (bottom) without biocides(a and c) and with silver/polyrhodanine decorated silica NPs (b and d).

3.3.2 Antimicrobial test under silver depletion condition

The decorated Ag NPs on the silica surface were releasable to the surrounding circumstances and kill the bacteria, while polyrhodanine kill the bacteria via direct contacting with bacterial membrane. Having a decorating with two distinct bactericidal mechanisms offers the opportunity to overcome certain disadvantages associated with each individual mechanism. For example, the continuous leaching of silver from the substrates will eventually lead to depletion. Recently, Alvarez *et al.* suggested that the antimicrobial activity of silver NPs majorly depends on the released Ag(I) ions.[48]

To understand the effect of silver depletion further, we used silver ion scavenger solution in antimicrobial test to inhibit the antimicrobial effect of silver NPs. Four different experimental types were designed: The SiO_2-Ag/PRh NPs dispersed solution with or without the silver ion scavenger which inhibit the antimicrobial activity of silver NPs; another type contains SiO_2-Ag NPs (without polyrhodanine) with or without silver ion scavenger. Each sample was inoculated with bacteria solution and incubated at 37 °C with shaking for 1 h. After then, same amount of aliquots were taken from

each tube and cultured on LB agar plates at 37 °C for 24 h. Silver ion scavenger containing solution was tested to confirm the toxicity of the scavenger solution to bacterial cells. Additionally, pristine silica NPs and thiol-silane treated silica NPs also tested under same experimental condition as comparative materials. As shown in Figure 13, blank solutions with and without Ag ion scavenger solution showed undistinguishable bacterial growth against both Gram-negative and –positive bacteria. Thus, the toxic effect of the scavenger solution can be neglected in our experimental condition. Additionally, the pristine silica and the thiol-silica NPs also does not showed specific antimicrobial properties against both bacteria. The SiO_2-Ag NPs presented high killing efficiency (>97%) due to Ag^+ release. When the silver ion scavenger was introduced, SiO_2-Ag NPs dispersed solution turned to dark brown, which indicated the released silver ions were captured. Notably, the Ag^+ scavenger added SiO_2-Ag NPs solution presented remarkably reduced bacteria killing efficiency against *E. coli* (24%) and *S. aureus* (7 %). Therefore, it can be considered that the antimicrobial activity of silver NPs can be effectively inhibited by addition of silver ion scavenger.

On the other hand, because of existence of polyrhodanine, SiO_2-Ag/PRh NPs were still able to maintain antimicrobial activity against *E. coli* (< 81%) and *S. aureus* (< 63%) after silver ion scavenger treatment. These data demonstrate that the SiO_2-Ag/PRh NPs containing both the release-killing silver and the contact-killing polyrhodanine have advantage as antimicrobial agent. Compared with Ag NPs solely decorated silica NPs, the SiO_2-Ag/PRh NPs can retain antimicrobial activity as a result of the existence of polyrhodanine even after the exclusion of the decorated silver.

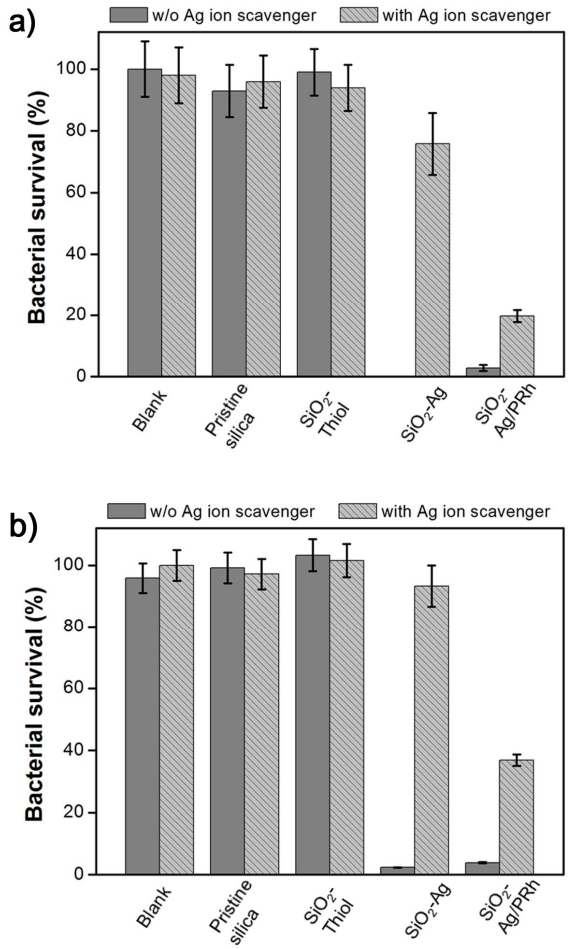

Figure 12 Antibacterial assessment of four different particles dispersed solution and blank water toward (a) *E. coli* and (b) *S. aureus* depending on with or without Ag ion scavenger in distilled water at 37 °C.

Chapter 4. Conclusion

Silver/polyrhodanine nanocomposite decorated silica NPs were successfully fabricated by chemical oxidation polymerization. The polymerization of rhodanine was preferentially occurred on the surface of Ag^+ ion-impregnated SiO_2. During the polymerization the Ag^+ ion reduced to metallic Ag NPs and consequentially silver-polyrhodanine composite NPs (*ca.* 7 nm) were formed on the surface of the SiO_2 NPs. A systematic evaluation of the antibacterial activity of the fabricated composite NPs presented excellent bactericidal properties against Gram-negative and – positive bacteria. Importantly, the SiO_2-Ag/PRh NPs retained antimicrobial activity under silver depletion condition due to the contact-active antimicrobial polyrhodanine. These results suggest that the SiO_2-Ag/PRh NPs can be a good potential candidate for a long-term useable antimicrobial agent.

References

[1] M. L. Cohen, *Nature* **2000**, *406*, 762.

[2] H. W. Boucher, G. H. Talbot, J. S. Bradley, J. E. Edwards Jr., D. Gilbert, L. B. Rice, M. Scheld, B. Spellberg and J. Bartlett, *Clin. Infect. Dis*. **2009**, *48*, 1.

[3] L. B. Rice, *Curr. Opin. Microbiol.* **2009**, *12*, 476.

[4] P. Tenke, C. R. Riedl, G. L. Jones, G. J. Williams, D. Stickler and E. Nagy, *Int. J. Antimicrob. Agents* **2004**, S67.

[5] S. Hou, H. Gu, C. Smith and D. Ren, *Langmuir* **2011**, *27*, 2686.

[6] L. Lu, F. H. Rininsland, S. K. Wittenburg, K. E. Achyuthan, D. W. McBranch and D. G. Whitten, *Langmuir* **2005**, *21*, 10154.

[7] S. Krishnan, N. Wang, C. K. Ober, J. A. Finlay, M. E. Callow, J. A. Callow, A. Hexemer, K. E. Sohn, E. J. Kramer and D. A. Fischer, *Biomacromolecules* **2006**, *7*, 1449.

[8] P. Kurt, L. Wood, D. E. Ohman and K. J. Wynne, *Langmuir* **2007**, *23*, 4719.

[9] H. V. R. Dias, K. H. Batdorf, M. Fianchini, H. V. K. Diyabalanage, S. Carnahan, R. Mulcahy, A. Rabiee, K. Nelson and L. G. Waasbergen, *J. Inorg. Biochem.* **2006**, *100*, 158.

[10] L. Balogh, D. R. Swanson, D. A. Tomalia, G. L. Hagnauer and A. T. McManus, *Nano Lett.* **2001**, *1*, 18.

[11] M. Ramstedt, N. Cheng, O. Azzaroni, D. Mossialos, H. J. Mathieu and W. T. S. Huck, *Langmuir* **2007**, *23*, 3314.

[12] U. Klueh, V. Wagner, S. Kelly, A. Johnson and J. D. Bryers, *J. Biomed. Mater. Res.* **2000**, *53*, 621.

[13] L. Timofeeva and N. Kleshcheva, *Appl. Microbiol. Biotechnol.* **2011**, *89*, 475.

[14] F. Siedenbiedel and J. C. Tiller, *Polymers* **2012**, *4*, 46.

[15] G. Seyfriedsberger, K. Rametsteiner and W. Kern, *Eur. Polym. J.* **2006**, *42*, 3383.

[16] A. M. Klibanov, *J. Mater. Chem.* **2007**, *17*, 2479.

[17] E.-R. Kenawy, S. D. Worley and R. Broughton, *Biomacromolecules* **2007**, *8,* 1359.

[18] M. L. W. Knetsch and L H. Koole, *Polymers* **2011**, *3*, 340.

[19] S. H. Hwang, J. Song, Y. Jung, O. Y. Kweon, H. Song and J. Jang, *Chem. Commun.* **2011**, *47*, 9164.

[20] J. R. Morones, J. L. Elechiguerra, A. Camacho, K. Holt, J. B. Kouri, J. T. Ramirez and M. J. Yacaman, *Nanotechnology* **2005**, *16*, 2346.

[21] G. Applerot, A. Lipovsky, R. Dror, N. Perkas, Y. Nitzan, R. Lubart and A. Gedanken, *Adv. Funct. Mater.* **2009**, *19*, 842.

[22] J. Song, H. Kong and J. Jang, *Chem. Commun.* **2009**, 5418.

[23] J. Song, H. Song, H. Kong, J.-Y. Hong and J. Jang, *J. Mater. Chem.* **2011**,

21, 19317.

[24] H.-J. Yen, S.-H. Hsu, and C.-L. Tsai, *Small* **2009**, *5*, 1553.

[25] P. V. Asharani, G. L. K. Mun, M. P. Hande and S. Valiyaveettil, *ACS Nano* **2009**, *3*, 279.

[26] J. C. Grunlan and J. K. Choi, *Biomacromolecules* **2005**, *6*, 1149.

[27] P. Dallas, V. K. Sharma and R. Zboril, *Adv. Colloid Interface Sci.* **2011**, *166*, 119.

[28] M. Lv, S. Su, Y. He, Q. Huang, W. Hu, D. Li, C. Fan and S.-T. Lee, *Adv. Mater.* **2010**, *22*, 5463.

[29] P. Dallas, J. Tucek, D. Jancik, M. Kolar, A. Panacek and R. Zboril, *Adv. Funct. Mater.* **2010**, *20*, 2347.

[30] H. Kong and J. Jang, *Langmuir* **2008**, *24*, 2051.

[31] Z. Li, D. Lee, X. Sheng, R. E. Cohen and M. F. Rubner, *Langmuir* **2006**, *22*, 9820.

[32] H. Kong and J. Jang, *Biomacromolecules* **2008**, *9*, 2677.

[33] H. Kong, J. Song and J. Jang, *Macromol. Rapid Commun.* **2009**, *30*, 1350.

[34] S. E. Skrabalak, L. Au, X. Li and Y. Xia, *Nat. Protoc.* **2007**, *2*, 2182.

[35] B. Lim and Y. Xia, *Angew. Chem. Int. Ed.* **2011**, *50*, 76.

[36] Y. Sun and Y. Xia, *Science* **2002**, *298*, 2176.

[37] A. Melaiye, Z. Sun, K. Hindi, A. Milsted, D. Ely, D. H. Reneker, C. A. Tessier and W. J. Youngs, *J. Am. Chem. Soc.* **2005**, *127*, 2285.

[38] H. Kong and J. Jang, *Chem. Commun*. **2006**, 3010.

[39] M. N. Nadagouda and R. S. Varma, *Macromol. Rapid Commun.*, **2009**, *30*, 1350.

[40] X. Yang and Y. Lu, *Mater. Lett.* **2005**, *59*, 2484.

[41] P. K. Khanna, N. Singh, S. Charan and A. K. Viswanath, *Mater. Chem. Phys.* **2005**, *92*, 214.

[42] K. L. Lee, Y. T. Moyasar, and G. O. Charles, *Appl. Environ. Microbiol.* **1989**, 3045.

[43] R.G. Pearson, *J. Am. Chem. Soc.* **1963**, *85*, 3533.

[44] S. Pandey, G. K. Goswami, and K. K. Nanda, *Int. J. Biol. Macromol.*, **2012**, *51*, 583.

[45] X. Sun, S. Dong and E. Wang, *Macromolecules* **2004**, *37*, 7105.

[46] X.Wang, J. C. Yu, C. Ho and A. C. Mak, *Chem. Commun.* **2005**, 2262.

[47] G. Kardas and R. Solmaz, *Appl. Surf. Sci.* **2007**, *253,* 3402.

[48] Z. Xiu, Q. Zhang, H. L. Puppala, V. L. Colvin and P. J. J. Alvarez, *Nano Lett.* **2012**, *12*, 4271.

국문요약

본 연구에서는 은/폴리로다닌 나노 입자가 박힌 실리카 나노 입자를 액상 중합을 통해 제조하였다. 은 이온을 흡착한 실리카 표면에서 로다닌 단량체의 중합이 진행되며, 이 과정에서 동시에 은 이온이 은 나노 입자로 환원된다. 이러한 산화중합을 통해 실리카 나노입자의 표면에 은/폴리로다닌 나노복합체가 형성되며 그 크기는 지름이 약 7 나노미터이다. 형성된 은 나노입자와 폴리로다닌의 존재는 적외선 분광광도계, 자외선-가시광선 분광광도계, X-선 광전자 분광기로 증명하였다. 제조된 은/폴리로다닌 나노 입자는 그람 음성균인 대장균과 그람 양성균인 포도상구균에 대해서 우수한 항균 능력을 보였다. 특히, 이 입자는 은이 고갈된 환경에서도 항균성 고분자인 폴리로다닌에 기인하여 장기간 사용 가능한 항균제로서의 가능성을 보여주고 있다.

주요어: 은 나노 입자, 폴리로다닌, 나노 복합체, 산화 중합, 항균

학 번: 2011-22915